Journal of Applied Polymer Science

Glycerol as high-permittivity liquid filler in dielectric silicone elastomers

P. Mazurek,[1] L. Yu,[1] R. Gerhard,[2] W. Wirges,[2] A. L. Skov[1]

[1]Danish Polymer Centre, Department of Chemical and Biochemical Engineering, Building 227, Technical University of Denmark, DK-2800 Kgs, Lyngby, Denmark

[2]Applied Condensed-Matter Physics, Institute of Physics and Astronomy, Faculty of Science, University of Potsdam, Karl-Liebknecht-Str. 24-25, 14476 Potsdam-Golm, Germany

Correspondence to: A. L. Skov (E-mail: al@kt.dtu.dk)

ABSTRACT: A recently reported novel class of elastomers was tested with respect to its dielectric properties. The new elastomer material is based on a commercially available poly(dimethylsiloxane) composition, which has been modified by embedding glycerol droplets into its matrix. The approach has two major advantages that make the material useful in a dielectric actuator. First, the glycerol droplets efficiently enhance the dielectric constant, which can reach astonishingly high values in the composite. Second, the liquid filler also acts as a softener that effectively decreases the elastic modulus of the composite. In combination with very low cost and easy preparation, the two property enhancements lead to an extremely attractive dielectric elastomer material. Experimental permittivity data are compared to various theoretical models that predict relative permittivity changes as a function of filler loading, and the applicability of the models is discussed. © 2016 Wiley Periodicals, Inc. J. Appl. Polym. Sci. **2016**, *133*, 44153.

KEYWORDS: crosslinking; dielectric properties; elastomers; sensors and actuators

Received 12 April 2016; accepted 30 June 2016

DOI: 10.1002/app.44153

INTRODUCTION

The concept of electromechanical transduction in polymeric materials was investigated by Wilhelm Conrad Röntgen already in 1880 in a simple experiment where a rubber band was actuated by sprayed-on charges that caused electrostatic forces across its thickness.[1,2] The early study became an inspiration for the research conducted nowadays on electroactive dielectric polymers, which intensified after 1990. Ever since, material scientists have worked on optimizing material properties and actuation conditions.[3–5]

It has been established that actuator performance strain in the thickness direction (s_z) depends on applied voltage (U), Young's modulus (Y), and initial thickness (d) of the elastomeric membrane and (last but not least) on the relative dielectric permittivity of the material (ε), as shown in eq. (1).[6] Here, ε_0 is the vacuum permittivity:

$$s_z = \frac{\varepsilon_0 \varepsilon}{Y}\left(\frac{U}{d}\right)^2 \quad (1)$$

Because of current, overly expensive power supply units, the risks of elastomer electrical breakdown, and a risk of exceeding the space-charge threshold (resulting in accelerated electrical aging), the applied voltage has to be kept at the lowest possible level.[7] Young's modulus and elastomer thickness are material properties that have to be adjusted for the respective applications. For an actuator or a generator, a dielectric polymer with the highest possible dielectric permittivity should be the best choice. Promising examples of such materials are polyurethanes[8] and poly(propylene oxide)[9] with dielectric constants of 6.2 and 5.6 at 1 kHz, respectively. In both cases, however, the materials suffer from relatively low breakdown strength and a short lifetime. For this reason, attention has shifted toward very soft, high dielectric constant polyacrylates and soft but low dielectric constant poly(dimethylsiloxane) (PDMS). The most widely applied representatives of the polyacrylates, the commercial Very High Bond (VHB) tapes from 3M, were recently reported to exhibit an impressively high power density of 280 W/kg.[10] Yet the prepared generator was capable of withstanding less than 10 cycles, after which the energy generation drastically decreased. Therefore, McKay *et al.*[11] asked whether it makes sense to conduct research on efficient but mechanically unstable polyacrylates. They suggested that investing time in a PDMS with lower energy density but much higher durability would contribute more significantly to the development of dielectric elastomers.

PDMS has over the years developed into a key candidate for dielectric actuators and generators because of its long lifetime, high durability, low viscous losses, high breakdown strength, and so on. Nevertheless, it suffers from a rather low dielectric

constant, which directly influences the performance of actuators or generators. There have been a number of publications in which the dielectric constant of PDMS was successfully enhanced through simply blending a PDMS prepolymer with high-permittivity fillers. This method, despite being the easiest and most intuitive, offers a broad range of possibilities due to an essentially unlimited selection of fillers, among which one can find magnesium niobate–lead titanate,[12] titanium dioxide,[13] graphite,[14] carbon nanotubes,[15] graphene,[16] and conductive polymers.[17] A more sophisticated method of increasing the permittivity has been presented by Madsen *et al.*,[18,19] who covalently linked dipolar molecules with high dielectric constant to the elastomer backbone via a novel type of chain extender. Nevertheless, none of the reported elastomers presently meets the requirements that are foreseen for a highly efficient, reliable and thus also commercially attractive dielectric elastomer. The indisputable need for materials improvement leads to many unconventional approaches for reaching a breakthrough in the development of dielectric elastomer actuators.[20]

In our recent papers,[21,22] liquids with high dielectric constant were suggested as fillers that are potentially capable of enhancing a material's dielectric constant. It was reported that water ($\varepsilon = 80$) incorporated and uniformly distributed within hydrophobic PDMS in the form of encapsulated discrete water droplets is capable of enhancing the dielectric constant of a given elastomer. On the other hand, the resulting composite material suffered from too-high film thickness, which greatly limited its range of applications. Furthermore, water, as a volatile substance, was gradually evaporating from the composite, which was additionally facilitated by the substantial gas permeability of PDMS.[23] Nevertheless, this approach, although having some drawbacks, proved our concept of polar liquids as useful high-permittivity fillers. The idea of using high-permittivity polar liquids as fillers in dielectric elastomers was also supported in a concept of generating water marbles that are responsive to high electric and magnetic fields.[24–27] Liquid marbles are often described as nonstick droplets coated with micrometer-sized hydrophobic particles.[28] The liquid marbles were proven to actuate upon exposure to sufficiently high electric fields. Due to dipole reorientation, water marbles change shape with the direction of an applied electric field. It has been postulated that the efficiency of actuation is directly related to the dielectric constant of the respective liquid.[29] That postulate let us to hypothesize that liquids might improve a dielectric elastomer actuation performance, provided that the liquid is nonvolatile and is incorporated into the elastomer in the form of discrete droplets.

Here, our recently developed silicone elastomer composite was investigated with respect to its possible use as an electroactive dielectric polymer. A cross section of the material is schematically presented in Figure 1. A detailed description of its preparation, as well as some relevant parameters and features, such as mechanical properties, can be found in our previous publication.[30] The glycerol-containing PDMS is tested in terms of the dielectric properties at high and low voltages. The approach offers a two-fold advantage over incorporating a high-permittivity liquid into a PDMS elastomer. First, the dielectric constant is significantly increased. Second, as shown in our previous paper,[30] zones of zero stress are introduced by embedding discrete liquid droplets into the elastomer matrix. This leads to an overall decrease of Young's modulus in the composite, which is expected to enhance its actuation performance.

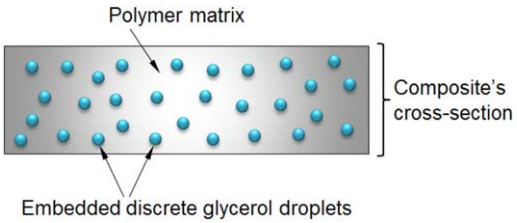

Figure 1. Schema of a glycerol–PDMS composite. Glycerol is embedded into a dielectric elastomer in the form of discrete droplets in order to avoid the formation of conductive pathways across the material. [Color figure can be viewed in the online issue, which is available at wileyonlinelibrary.com.]

EXPERIMENTAL

Materials

The two-component Sylgard 184 (abbreviated as S184) silicone kit and the volatile methylsiloxane fluid OS-20 (abbreviated as OS20) were purchased from Dow Corning, Midland, Michigan, US. Powersil XLR 630 A/B (abbreviated as XLR630) was obtained from Wacker Chemie, Burghausen, Germany, AG. Both silicones are platinum-catalyzed hydrosilylation addition-cured systems reinforced with silica particles. A food-grade glycerol was kindly provided by Emmelev, Otterup A/S Denmark and was used as received. Tween 20, a polysorbate-based surfactant, was obtained from Sigma Aldrich, Broendby, Denmark. Two different methyl-terminated poly(dimethylsiloxane-*b*-ethylene oxide) surfactant-like diblock copolymers were purchased from Polysciences, Warrington, PA, Inc., where a lower molecular weight PDMS–poly(ethylene glycol) (PEG) copolymer ($M = 600$ g/mol) and a higher molecular weight PDMS–PEG copolymer ($M = 3000$ g/mol) had estimated molar ratios of PEG to PDMS blocks of 25:75 and 20:80, respectively. The PEG blocks were estimated to have a molecular weight of $M = 400$ g/mol. The copolymer specifications were provided by the supplier. All chemicals were used as received with no further purification.

Sample Preparation

All composite prepolymer compositions were prepared via mixing all compounds with a dual asymmetric centrifuge SpeedMixer, High Wycombe, UK, DAC 150 FVZ-K. The S184 was mixed in a ratio of 10:1 as recommended by the supplier. Subsequently, glycerol was added to the prepolymer, followed by vigorous stirring with the speed-mixer at 3500 r.p.m. for 5 minutes. The glycerol–PDMS prepolymer emulsion was cast onto a metal mold with a 1-mm-thick spacer and cured for 1 h at 80 °C. Afterwards, the samples were kept at room temperature for at least 2 days prior to the measurements in order to ensure that eventual postcuring was completed. Because of the very low vapor pressure, an eventual evaporation of glycerol from the produced films is neglected. The amounts of incorporated glycerol by mass and the corresponding volume fractions are given in Table I.

The Powersil XLR 630 was mixed in a ratio of 1:1 by weight, as recommended by the manufacturer, which was followed by the

Table I. Glycerol–S184 Formulations with Corresponding Volume Fractions

Sample name[a]	Amount of glycerol (phr)[b]	Volume fraction of glycerol in sample
G0_S184	0	0
G10_S184	10	0.075
G20_S184	20	0.141
G40_S184	40	0.246
G60_S184	60	0.329
G80_S184	80	0.395
G100_S184	100	0.450
G120_S184	120	0.495

Volume fractions for glycerol–XLR630 formulations are slightly different because of the higher density of XLR630.
[a] Sample names were formed using the pattern GX_Y_Z, where G and X denote glycerol and the amount of glycerol phr added to a PDMS prepolymer, respectively; Y corresponds to the PDMS composition employed; and Z indicates supplementary components (in the approach discussed here, it corresponds to the thinning fluid OS20).
[b] The abbreviation "phr" used for describing glycerol content in all compositions corresponds to glycerol amount by weight per hundred weight parts of silicone rubber.

addition of glycerol. Subsequently, 40 phr of OS20 fluid was added to the system. This low molecular weight, low viscosity, volatile and PDMS-prepolymer-miscible substance effectively decreases the viscosity of the silicone compositions, making them much easier to process. The speed-mixed compositions (3500 r.p.m. for 5 minutes) were cast onto a metal mold as in the previous case. Here again, the samples were cured for 1 h at 80 °C. Subsequently, the samples were kept at room temperature for at least 7 days in order to ensure complete crosslinking of the material as well as evaporation of the remaining OS20.

Samples with addition of a surfactant were prepared in the same way as the glycerol–S184 composites, adding the desired amounts of surfactant before speed-mixing.

Methods

A Field Electron and Ion Co., Hillsboro, Oregon (FEI) Inspect scanning electron microscope (SEM) was used to obtain images of typical cross sections of fully crosslinked samples. A Novocontrol, Montabaur, Germany, broadband dielectric spectrometer was employed to determine the real and imaginary parts of the complex permittivities as well as the conductivities on the composite specimens. Disk-shaped samples with a diameter of 20 mm and a thickness of around 1 mm were subjected to an AC voltage of 1 V amplitude in the frequency range between 10^{-1} and 10^{6} Hz. A broadband dielectric spectrometer Novocontrol Alpha-A, equipped with a high-voltage booster HVB1000, was used to investigate the dielectric response of samples as a function of the applied voltage. Specimens were tested in a frequency range between 10^{-1} and 10^{4} Hz (a narrower frequency range than in the case of the 1 V AC measurements, due to technical limitations). When discussing the resulting dielectric permittivities of the composites, the values at 1 kHz are used.

RESULTS AND DISCUSSION

SEM Analysis of Glycerol–PDMS Composites

Cross sections of crosslinked composites were investigated by SEM. Images I and II, presented in Figure 2, correspond to the cross sections of samples G20_S184 and G80_S184, respectively. As can be seen, the droplet concentration becomes higher with an increasing amount of glycerol. However, the average droplet size remains almost unchanged. Furthermore, it was observed that when increasing the glycerol/PDMS ratio, a threshold concentration is finally reached (G130_S184), above which a droplet-like morphology is no longer present in the crosslinked material. As discussed previously, a network of interconnected glycerol channels is obtained instead, which leads to higher-conductivity paths in the material.[30] Therefore, samples with more than 120 phr of glycerol are not discussed here.

The addition of the thinning agent to XLR630 was shown to allow for the incorporation of significant amounts of glycerol (up to 120 phr) into the PDMS matrix and also facilitated processability. Without the addition of the diluting OS20, a maximum possible glycerol loading of 40 phr was observed. Above this limit, the glycerol–XLR630 prepolymer emulsions had a very broad size distribution of glycerol droplets, and the mixtures were phase-separated even after extended mixing. As depicted in Figure 2 (images III and IV), the morphology of spherical droplets embedded within the PDMS matrix is not present in samples G20_XLR630 and G80_XLR630. Elongated, ellipsoid-like glycerol droplets were formed instead. It is hypothesized that this is an effect of using the thinning agent OS20, which was rapidly evaporating from the hydrophobic phase of the samples during the crosslinking process. Intuitively, the fluid was evaporating upward, which led to the orientation of the glycerol droplets in the direction of evaporation. The longest semi-axis of the ellipsoid-like droplets was proved, via SEM analysis, to be parallel to the theoretical direction of evaporation. Despite this anomaly, glycerol droplets were successfully encapsulated within the XLR630 PDMS composition, which was substantiated further in the dielectric spectroscopy results. Adding thinning fluids is a common practice, since it greatly simplifies the processability of high-viscosity polymeric compositions. Importantly, the SEM analysis showed that introducing thinning agents might lead to anisotropy in the resulting composite material, which might also deteriorate the ultimate properties of the material and eventually limit its usefulness. Therefore, a proper balance between evaporation rate and PDMS curing conditions has to be found for each PDMS system.

Dielectric Spectroscopy

Broadband dielectric spectroscopy tests were performed in order to determine the dielectric properties of compositions with various amounts of glycerol incorporated. In this study, a two-phase system is described in which a higher-conductivity material is distributed within a lower-conductivity material in the form of discrete droplets. The droplets were expected to act as a high-permittivity filler uniformly distributed throughout the dielectric polymer matrix. Since the material is based on a glycerol–PDMS emulsion, it can be assumed that the glycerol droplets are effectively encapsulated within a PDMS insulating layer. Intuitively, this effect should eliminate the probability of the formation of conductive paths throughout the material, and consequently the

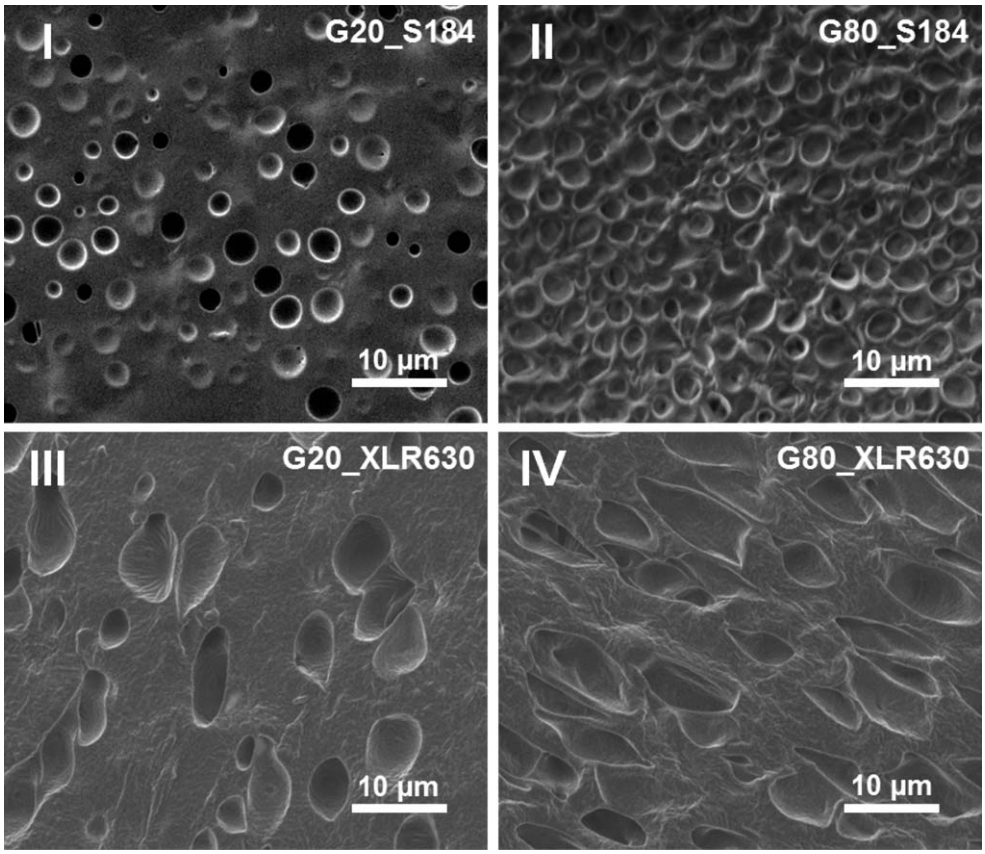

Figure 2. SEM images of cured glycerol–PDMS composite cross sections.

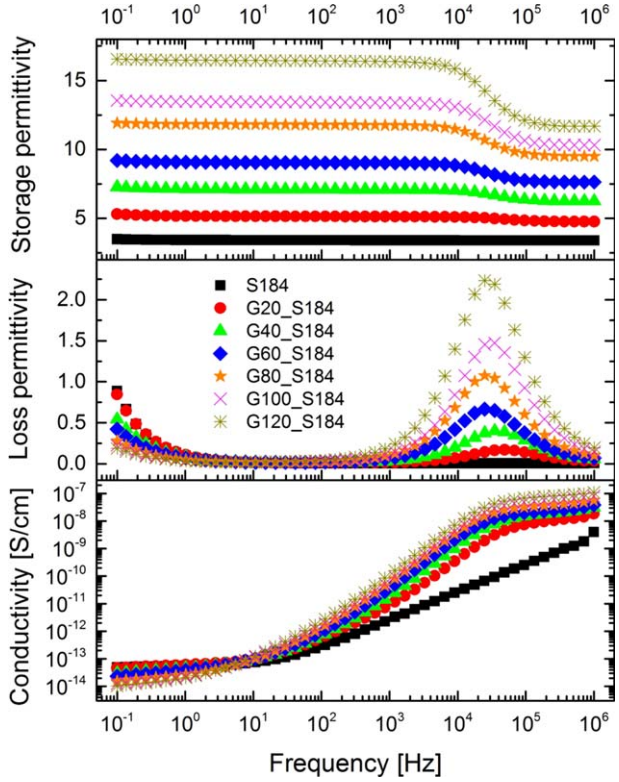

Figure 3. Storage permittivity, loss permittivity, and AC conductivity of various glycerol–S184 composites at room temperature. [Color figure can be viewed in the online issue, which is available at wileyonlinelibrary.com.]

conductivity should not be affected by increased amounts of filler. The advantages of filler encapsulation have been thoroughly explained by other groups.[31]

As can be seen in Figure 3, a significant increase in dielectric constant is observed with increasing glycerol loading. The permittivity at 1 kHz increases from around 3.3 for neat Sylgard 184 up to around 16 for a sample of G120_S184. Importantly, already a composition with 20 phr of the filler exhibits a significant enhancement of permittivity compared to the neat sample. Consequently, the G20_S184 and G40_S184 samples have dielectric constants of 5.1 and 7.1, respectively, at 1 kHz. It should be noted that all of the curves for samples with incorporated glycerol exhibit a characteristic inflection in the frequency region between 10^4 and 10^6 Hz, which might be evidence of a dipolar relaxation of the high-permittivity filler. The higher the glycerol loading, the steeper the relaxation step, and, in line with the increasing height of the relaxation step, a characteristic peak in the dielectric loss occurs in the same frequency region. This is an additional indication of the presence of a dipolar relaxation. Importantly, dielectric losses are considered to be exceptionally low for all of the investigated compositions, reaching a maximum of around 2.5 in the higher frequency region. As expected, conductivities are not significantly altered by increasing additions of filler, which justifies the concept of glycerol encapsulation. The conductivity curves also exhibit characteristic slope changes that correspond to the postulated dipole relaxation.

XLR630-based samples also exhibit significant enhancements of their dielectric constants (see Figure 4), which are even more

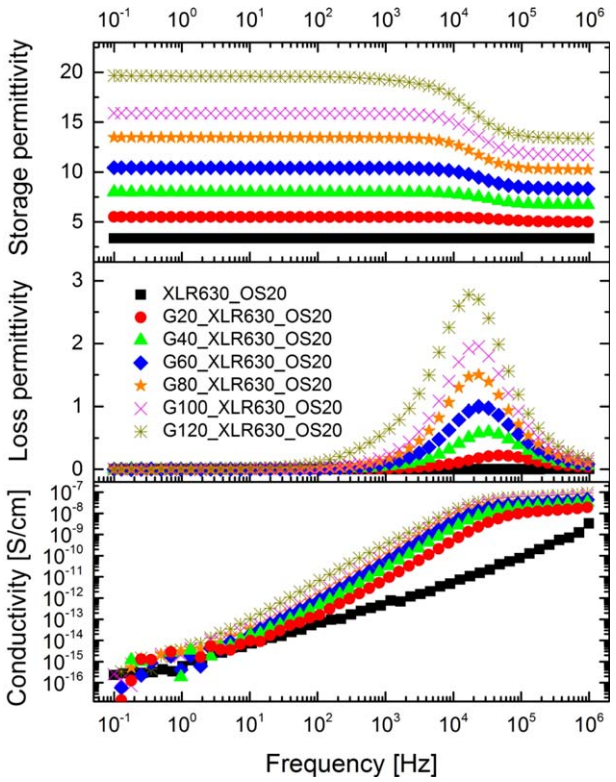

Figure 4. Storage permittivity, loss permittivity, and AC conductivity of various glycerol–XLR630 composites at room temperature. [Color figure can be viewed in the online issue, which is available at wileyonlinelibrary.com.]

prominent than in the case of S184. A maximum dielectric constant of around 20 was reached with the G120_XLR630 sample. S184 and XLR630 have comparable dielectric constants, and thus the higher values for XLR630-based composites are unexpected. The thinning agent is not anticipated to influence the dielectric constant directly, because of its presumed complete evaporation. It can be hypothesized that the difference comes from the shape of the embedded filler, as this might alter interactions between adjacent glycerol droplets.

The gradual increase in relative permittivity as a function of filler concentration has also been compared to various theoretical models predicting the behavior of composites of low-permittivity polymers blended with high-permittivity fillers. All models were developed for binary systems, where the inclusions are spherical. For this reason, only composites based on Sylgard 184 were considered, as the filler can be assumed to be spherical only in this case. First, presuming the existence of approximate lower [eq. (2)] and upper [eq. (3)] limits for such binary systems, a simple mixing rule is chosen[32]:

$$\varepsilon_{c,\min} = \frac{\varepsilon_m \varepsilon_f}{\varepsilon_m \nu_f + \varepsilon_f \nu_m} \quad \text{and} \tag{2}$$

$$\varepsilon_{c,\max} = \varepsilon_m \nu_m + \varepsilon_f \nu_f \tag{3}$$

where ε_c, ε_m, and ε_f are the permittivities of the composite, the matrix, and the filler, respectively, while v_m and v_f are the volume fractions of matrix and filler in the binary composites. The experimental data fit well within the limits of the model. Yet, a more accurate model is necessary in order to follow more precisely the observed trends. More sophisticated predictions can be obtained with one of the earliest mixing formulas, the so-called Maxwell–Garnett (M&G) eq. (4), which holds for a relatively broad range of volume fractions[33,34]:

$$\varepsilon_c = \varepsilon_m \left[1 + \frac{3\nu_f (\varepsilon_f - \varepsilon_m)}{\nu_m (\varepsilon_f - \varepsilon_m) + 3\varepsilon_m} \right] \tag{4}$$

Corrections to the aforementioned equations were introduced by Bruggeman.[35] His model covers inclusion volume fractions up to 0.5 and is therefore frequently used for describing composites with very high filler loadings.[12] The model may even be applied after the formation of agglomerates, provided the percolation threshold is not exceeded. The equation is usually given in the following form:

$$\frac{\varepsilon_f - \varepsilon_c}{\varepsilon_c^{1/3}} = \frac{(1-\nu_f)(\varepsilon_f - \varepsilon_m)}{\varepsilon_c^{1/3}} \tag{5}$$

Subsequently, the applicability of the well-known Jayasundere–Smith (J&S) model in the present case was tested.[36,37] In this model, it is assumed that the dielectric constant of the inclusions is substantially higher than that of a dielectric continuum. Additionally, the formula takes into account polarization-based interactions between adjacent particles. Intuitively, the probability of particle–particle interactions is much higher for high filler loadings. Therefore, it is expected that the experimental data will fit better to the predictions from this model, especially at very high inclusion volume fractions. The model is represented by the following equation:

$$\varepsilon_c = \frac{\varepsilon_m \nu_m + \varepsilon_f \nu_f \frac{3\varepsilon_m}{(2\varepsilon_m + \varepsilon_f)} \left[1 + 3\nu_f \frac{(\varepsilon_f - \varepsilon_m)}{2\varepsilon_m + \varepsilon_f} \right]}{\nu_m + \nu_f \frac{3\varepsilon_m}{(2\varepsilon_m + \varepsilon_f)} \left[1 + 3\nu_f \frac{(\varepsilon_f - \varepsilon_m)}{2\varepsilon_m + \varepsilon_f} \right]} \tag{6}$$

Last but not least, a model proposed by Poon and Shin (P&S) [eq. (7)] is considered. The formula was developed in order to find a model that may fit as broad a range of systems as possible.[38] The formula is not limited to the case of $\varepsilon_f \gg \varepsilon_m$ [as with eq. (6), Jayasundere–Smith] and covers even situations where $\varepsilon_f < \varepsilon_m$. Furthermore, the simplicity of eq. (7) is one of its strengths. As the authors argue, more complicated nonlinear equations [such as eq. (5), Bruggeman] have limited use in situations where a simpler formula may be employed:

$$\varepsilon_c = \varepsilon_m + \frac{\nu_f (\varepsilon_f - \varepsilon_m)}{\nu_f + \nu_m \frac{\varepsilon_f + 2\varepsilon_m - \nu_f (\varepsilon_f - \varepsilon_m)}{3\varepsilon_m}} \tag{7}$$

Experimental values of the storage permittivity at a frequency of 1 kHz were used for comparisons between the various models. Between 0.1 Hz and 10 kHz, the curves exhibit a plateau, so the analysis may be assumed to be valid for a broader frequency range. As can be seen in Figure 5, the model proposed by Jayasundere and Smith fits the experimental data in the best way. The theoretical estimate fits the data from lower glycerol loadings up to loadings of around 100 phr, and the value at 120 phr of glycerol deviates only slightly from the model curve. As discussed before, the material becomes more conductive at very high inclusion loadings (>120 phr). Here, the deviation is not significant but might be attributed to the formation of a continuous glycerol phase and of conductive pathways. All models have been developed for 0–3 composites (spherical filler

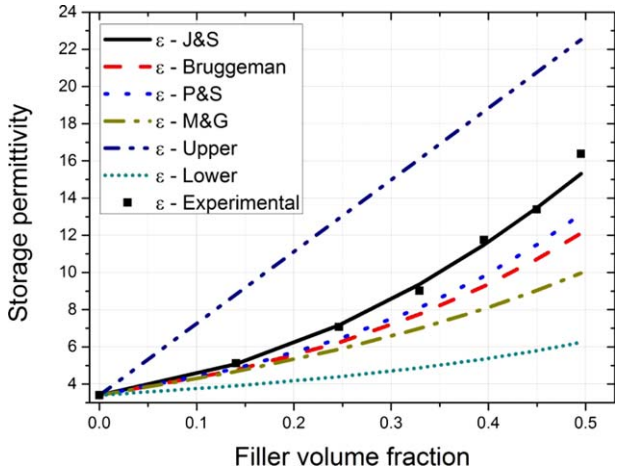

Figure 5. Experimental data and theoretical estimate of the relative permittivity at 1 kHz as a function of the glycerol loading in the composites. [Color figure can be viewed in the online issue, which is available at wileyonlinelibrary.com.]

particles embedded in a continuous matrix), and thus the validity of the equations is restricted to filler loadings below 120 phr.

As can be seen in Figures 3 and 4, the conductivities in the lower frequency region of the glycerol–PDMS composites do not change significantly with increasing glycerol loadings. However, the SEM analysis showed that the insulating layers between the glycerol droplets become thinner for increasing amounts of filler, as expected. Therefore, the chances for charge migration between the droplets become higher. Although higher conductivities are not to be expected at 1 V, tests at higher voltages were performed in order to validate the usefulness of the material for high-voltage applications. Several samples of G100_S184 and G100_XLR630_OS20 were subjected to increasing AC voltages, and the results are presented in Figure 6. The conductivity of G100_S184 increases significantly with increasing voltage, while the conductivity of G100_XLR630_OS20 remains almost unaffected. The conductivity of unmodified XLR630, tested at 1 V, is lower than that of S184 under the same conditions (see Figures 3 and 4). As the amount of inclusions is exactly the same in both samples, it can be concluded that the type of matrix is essential for the conductivity of glycerol–PDMS composites. Intuitively, materials with higher resistivity (resistivity is the reciprocal of conductivity) will insulate the glycerol droplets more efficiently and block charge transfer between adjacent spheres. Ultimately, the probability of forming conductive paths will be considerably restricted in a dielectric matrix with higher resistivity.

As discussed, the thinner the insulating layer between the inclusion droplets, the higher the conductivity. This is also demonstrated by the results presented in Figure 7, in which the conductivities of samples G80_S184 and G100_S184 are compared. As can be observed, the conductivity of the sample with 80 phr is not influenced by a voltage increase from 1 V to 350 V, whereas for the sample with 100 phr, the conductivity drastically increases at 350 V. This suggests the existence of a required minimum spacing for separating and insulating adjacent glycerol droplets from each other. It is believed that the threshold for the shell thickness would be lower in materials with higher electrical resistivity.

Modification of Droplet Size and Its Influence on the Dielectric Constant of Glycerol–PDMS Composites

In the previous section, well-known theoretical models for predicting the dielectric constants of composites were evaluated. Additional reports that emphasize the necessity of considering a polymer–filler interphase as an additional factor influencing the final dielectric constant of a material can be found in the literature.[39,40] Furthermore, Vo and Shi[41] discuss the presence of a molecular polarizability at the filler–polymer interphase, which might also influence the resulting permittivity. As the filler–polymer interphase increases in line with a decrease in filler size at a given loading, it is expected that a change in relative permittivity will be observed.

Various surfactants in different amounts were added to the G10_S184 pre-elastomer composition, and their influence on droplet diameters was investigated. First, 1-mm-thick samples of PDMS containing 10 phr of glycerol with the addition of Tween 20 (a glycerol-miscible, polysorbate-based surfactant) were prepared according to the standard procedure used in this

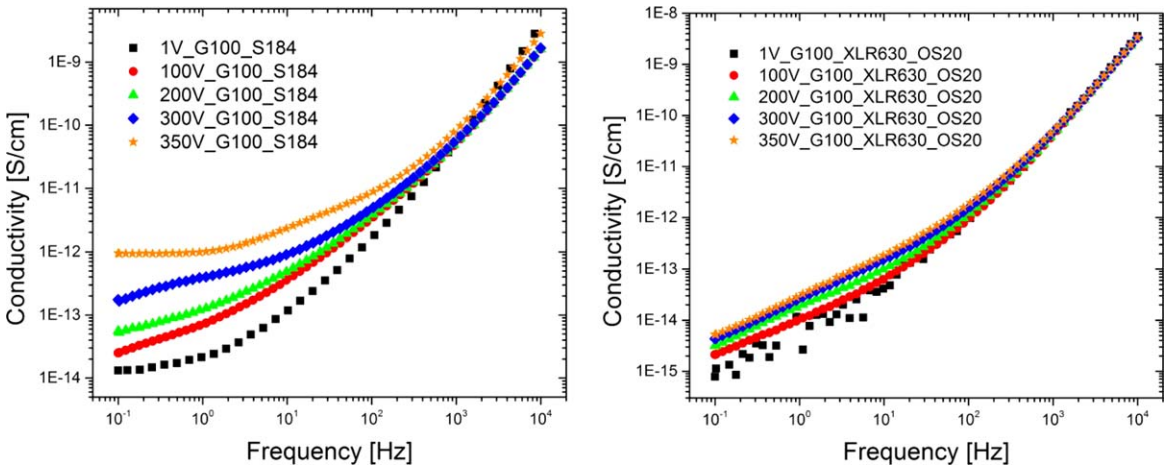

Figure 6. Conductivities of composites based on S184 (left) and XLR630 (right), containing 100 phr of glycerol for various AC voltages at room temperature. [Color figure can be viewed in the online issue, which is available at wileyonlinelibrary.com.]

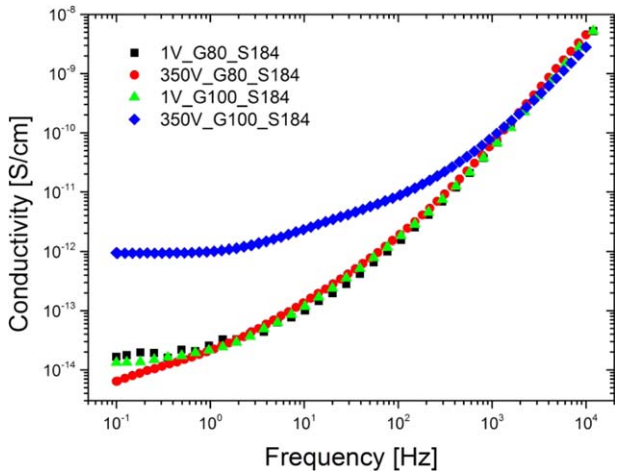

Figure 7. Conductivity of various glycerol–S184 composites for 1 V and 350 V, respectively, at room temperature. [Color figure can be viewed in the online issue, which is available at wileyonlinelibrary.com.]

study. SEM images of samples with 0.1 and 5 parts by weight of the surfactant are shown in Figure 8(a). The data presented in Figure 8(b) indicate that an increasing amount of surfactant in a composition leads to the formation of smaller glycerol droplets, along with a narrower size distribution. The average droplet diameter decreases from 2.3 μm for the nonsurfactant sample to 0.8 μm for the highest Tween 20 loading investigated here. The dielectric constant increased from 4.2 for pure G10_S184 to 5.0 with the addition of 5 phr of Tween 20. Nevertheless, the steepest increase was observed for smaller amounts of Tween 20, which correlates well with the stronger decrease in droplet diameter at lower surfactant loadings. Remarkably, the dielectric constant of the sample G20_S184 was found to be 5.1, whereas the sample G10_S184 with the addition of only 3 phr of Tween 20 reached a dielectric constant of 4.9. This implies that a strong dependence exists between dielectric constant and filler size, that is, that the space-charge motion within the composite is more remarkable in the S184 composites.

A significant decrease in the average droplet diameter was also observed after incorporating two PEG–PDMS surfactants (block-copolymer-based surfactants with molecular weights of 400 g/mol and 3000 g/mol, respectively, with comparable ratios between the PEG and the PDMS blocks) into the G10_S184 composition. The influence on the droplet diameters was similar to the effects of Tween 20; however, no clear increase in the dielectric constant was observed on these samples.

The aim of this approach was to investigate how the volume of the filler–polymer interphase influences the dielectric constant of composites. The contradictory results indicate that the properties vary with the constituents that form the interphase, suggesting a high complexity of the processes that occur in the interphase. It is therefore necessary to consider each system separately.

It has to be stressed that the diameters obtained from evaluating the cross sections do not correspond to the actual droplet diameters, as it is not possible to prepare sample cross sections by cutting each inclusion droplet through its respective center. Nevertheless, for a comparative study, the present approach is considered to be sufficiently accurate.

CONCLUSIONS

The use of glycerol–PDMS green elastomers and their potential applicability as dielectric elastomers were proposed, investigated, and discussed. This novel class of materials has been proven to exhibit high dielectric constants strongly depending on the glycerol loading. Furthermore, the glycerol–PDMS composites were shown to exhibit very low dielectric losses. The composites were assessed by means of some of the most popular theoretical models that predict changes in relative permittivities as a function of filler content. The results show that the formula suggested by Jayasundere and Smith fits the experimental data best. The J&S theory takes into account interactions between adjacent filler particles, which intuitively intensify at higher glycerol loadings. This factor is considered to be the main advantage of the model.

The high-voltage dielectric spectroscopy measurements indicate that the conductivity tends to increase with increasing voltages and filler loadings. Nonetheless, the experimental results

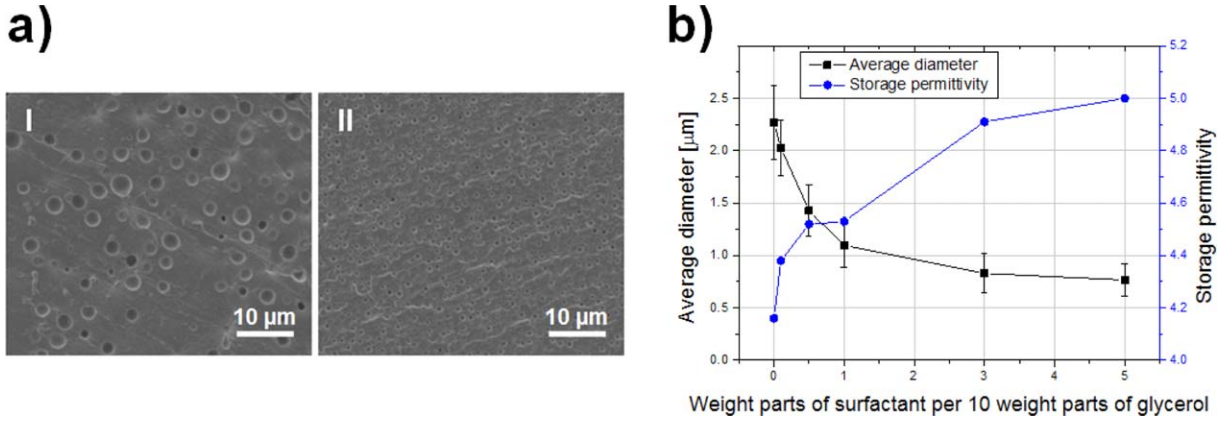

Figure 8. Effect of surfactant on droplet size. (a) SEM images of cured samples G10_S184 with 0.1 (I) and 5 (II) phr of Tween 20. The scale bars in both images correspond to 10 μm. (b) Average glycerol droplet diameter and storage permittivity at 1 kHz as a function of surfactant content in various Tween 20–glycerol–PDMS composites. [Color figure can be viewed in the online issue, which is available at wileyonlinelibrary.com.]

indirectly also show that this problem can be overcome by using the best possible dielectric material as a matrix for composites. It is believed that a highly resistive dielectric matrix would be capable of preventing charge transfer between adjacent glycerol droplets. This is especially important at high filler loadings, where the distances between the droplets become very small.

The novel elastomer material exhibits several interesting features from the perspective of dielectric-elastomer transducer development, with a very high dielectric constant and a tunable elastic modulus being the two most important ones. The simplicity of preparation and the variety of potential candidates for the matrix and the inclusions are other key aspects of the new concept.

ACKNOWLEDGMENTS

The authors acknowledge funding from Innovationsfonden Denmark and from the Deutsche Forschungsgemeinschaft (DFG) and the European Union (EU) for equipment.

REFERENCES

1. Röntgen, W. C. *Ann. Phys. Chem.* **1880**, *11*, 771.
2. Keplinger, C.; Kaltenbrunner, M.; Arnold, N.; Bauer, S. *Proc. Natl. Acad. Sci. U. S. A.* **2010**, *107*, 4505.
3. Pelrine, R.; Kornbluh, R.; Joseph, J.; Heydt, R.; Pei, Q.; Chiba, S. *Mater. Sci. Eng. C* **2000**, *11*, 89.
4. Zhenyi, M.; Scheinbeim, J. I.; Lee, J. W.; Newman, B. A. *J. Polym. Sci., Part B: Polym. Phys.* **1994**, *32*, 2721.
5. Shkel, Y. M.; Klingenberg, D. J. *J. Appl. Phys.* **1996**, *80*, 4566.
6. Pelrine, R. *Science* **2000**, *287*, 836.
7. Kochetov, R.; Tsekmes, I. A.; Morshuis, P. H. F. *Smart Mater. Struct.* **2015**, *24*, 075019.
8. Gallone, G.; Galantini, F.; Carpi, F. *Polym. Int.* **2010**, *59*, 400.
9. Goswami, K.; Galantini, F.; Mazurek, P.; Daugaard, A. E.; Gallone, G.; Skov, A. L. *Smart Mater. Struct.* **2013**, *22*, 115011.
10. Huang, J.; Shian, S.; Suo, Z.; Clarke, D. R. *Adv. Funct. Mater.* **2013**, *23*, 5056.
11. McKay, T. G.; Rosset, S.; Anderson, I. A.; Shea, H. *Smart Mater. Struct.* **2015**, *24*, 015014.
12. Gallone, G.; Carpi, F.; De Rossi, D.; Levita, G.; Marchetti, A. *Mater. Sci. Eng. C* **2007**, *27*, 110.
13. Vudayagiri, S.; Zakaria, S.; Yu, L.; Hassouneh, S. S.; Benslimane, M.; Skov, A. L. *Smart Mater. Struct.* **2014**, *23*, 105017.
14. Daugaard, A. E.; Hassouneh, S. S.; Kostrzewska, M.; Bejenariu, A. G.; Skov, A. L. *Proc. SPIE* **2013**, *8687*, 868729.
15. Goswami, K.; Daugaard, A. E.; Skov, A. L. *RSC Adv.* **2015**, *5*, 12792.
16. Javadi, A.; Xiao, Y.; Xu, W.; Gong, S. *J. Mater. Chem.* **2012**, *22*, 830.
17. Carpi, F.; Gallone, G.; Galantini, F.; De Rossi, D. *Adv. Funct. Mater.* **2008**, *18*, 235.
18. Madsen, F. B.; Daugaard, A. E.; Hvilsted, S.; Benslimane, M. Y.; Skov, A. L. *Smart Mater. Struct.* **2013**, *22*, 104002.
19. Madsen, F. B.; Yu, L.; Daugaard, A. E.; Hvilsted, S.; Skov, A. L. *RSC Adv.* **2015**, *5*, 10254.
20. Madsen, F. B.; Daugaard, A. E.; Hvilsted, S.; Skov, A. L. *Macromol. Rapid Commun.* **2016**, *37*, 378.
21. Mazurek, P.; Daugaard, A. E.; Skolimowski, M.; Hvilsted, S.; Skov, A. L. *RSC Adv.* **2015**, *5*, 15379.
22. Mazurek, P.; Hvilsted, S.; Skov, A. L. *Proc. SPIE* **2014**, *9056*, 90562T.
23. Zhang, Y.; Ishida, M.; Kazoe, Y.; Sato, Y.; Miki, N. *IEEJ Trans. Electr. Electron. Eng.* **2009**, *4*, 442.
24. Bormashenko, E. *Soft Matter* **2012**, *8*, 11018.
25. Bormashenko, E.; Pogreb, R.; Stein, T.; Whyman, G.; Schiffer, M.; Aurbach, D. J. *Adhes. Sci. Technol.* **2011**, *25*, 1371.
26. Xue, Y.; Wang, H.; Zhao, Y.; Dai, L.; Feng, L.; Wang, X.; Lin, T. *Adv. Mater.* **2010**, *22*, 4814.
27. Zhao, Y.; Xu, Z.; Parhizkar, M.; Fang, J.; Wang, X.; Lin, T. *Microfluid. Nanofluidics* **2012**, *13*, 555.
28. Aussillous, P.; Quéré, D. *Nature* **2001**, *411*, 924.
29. Bormashenko, E.; Pogreb, R.; Balter, R.; Gendelman, O.; Aurbach, D. *Appl. Phys. Lett.* **2012**, *100*, 151601.
30. Mazurek, P.; Hvilsted, S.; Skov, A. L. *Polymer* **2016**, *87*, 1.
31. Hu, W.; Zhang, S. N.; Niu, X.; Liu, C.; Pei, Q. *J. Mater. Chem. C* **2014**, *2*, 1658.
32. Carpi, F.; De Rossi, D.; Kornbluh, R.; Pelrine, R.; Sommer-Larsen, P. Dielectric Elastomers as Electromechanical Transducers; Elsevier: Amsterdam, **2008**; p 55.
33. Garnett, J. C. M. *Philos. Trans. R. Soc. A Math. Phys. Eng. Sci.* **1906**, *205*, 237.
34. Tuncer, E.; Gubański, S. M.; Nettelblad, B. *J. Appl. Phys.* **2001**, *89*, 8092.
35. Nelson, S. O.; You, T. S. *J. Phys. D. Appl. Phys.* **1990**, *23*, 346.
36. Jayasundere, N.; Smith, B. V. *J. Appl. Phys.* **1993**, *73*, 2462.
37. Jayasundere, N.; Smith, B. V.; Dunn, J. R. J. *Appl. Phys.* **1994**, *76*, 2993.
38. Poon, Y. M.; Shin, F. G. *J. Mater. Sci.* **2004**, *39*, 1277.
39. Ezzat, M.; Sabiha, N. A.; Izzularab, M. *Appl. Nanosci.* **2013**, *4*, 331.
40. Todd, M. G.; Shi, F. G. *J. Appl. Phys.* **2003**, *94*, 4551.
41. Vo, H. T.; Shi, F. G. *Microelectronics J.* **2002**, *33*, 409.